

A Novel PIFA Design for SAR Reduction in 5G Networks to Analyze the RF Shield Impact

Ashok Kumar Penta

Department of EECE, GITAM School of Technology, GITAM deemed to be University, Andhra Pradesh, India
ashok.pentaace@gmail.com

Ch. R. Phani Kumar

Department of EECE, GITAM School of Technology, GITAM deemed to be University, Andhra Pradesh, India
rchintal2@gitam.edu

Received: 3 March 2024 | Revised: 19 March 2024 | Accepted: 21 March 2024

Licensed under a CC-BY 4.0 license | Copyright (c) by the authors | DOI: <https://doi.org/10.48084/etasr.7184>

ABSTRACT

Fifth Generation (5G) Technology, representing the latest advancement in wireless communication networks, has brought attention to the rising concerns regarding Specific Absorption Rate (SAR) due to temperature fluctuations. The negative impacts of SAR, particularly in the context of mobile users' head exposure, have prompted the exploration of effective mitigation strategies. This article introduces a novel approach, employing a Planar Inverted F-Antenna (PIFA) operating at 26 GHz, with the integration of RF shields, specifically a flexible ferrite sheet and a foam absorber, aimed at reducing SAR in the human head. Dosimetry investigations, conducted at frequencies exceeding 26 GHz, reveal that SAR values without shielding materials (1.59 W/kg) approach the safety limit of SAR. The incorporation of ferrite and foam absorber leads to SAR reductions of 1.53 and 1.48 W/kg, respectively. Notably, the proposed antenna demonstrates significant SAR Reduction Factor (SRF) values, particularly at 5G network frequencies (26 GHz). Comparative analysis highlights the superior performance of the foam absorber across various parameters. The prototype of the proposed antenna has been fabricated and subjected to testing, affirming its potential for alleviating SAR in the context of 5G technology.

Keywords-SAR;5G Networks;PIFA;SRF

I. INTRODUCTION

5G technology has recently gained popularity in the telecommunication sector. Compared to the 4G network that is currently available, this network is quicker and able to handle more connected devices. The 5G antennas should be compact and lightweight given that they are typically used in portable devices like tablets and smart phones. It is crucial to assess any negative impacts on health brought on by electromagnetic fields [1] given the rapid expansion of systems based on millimeter wave (mmW) technologies. Due to the exposure to mmW radiation, there is an urgent need to research how electromagnetic energy is absorbed in human tissues. Radiation exposure from mobile phones has been linked to major health issues, such as cancer, brain tumors, heart illness, blood pressure irregularities, and skin diseases. EM wave absorption by the human body is measured employing the Specific Absorption Rate (SAR). Several safety measures that are implemented in new antenna releases should be taken into consideration while minimizing the SAR. Reduced antenna size, increased antenna compactness, and augmented antenna robustness are some of these safety measures. Achieving SAR values within the internationally allowed limit is one of the

most important factors to be considered when designing an antenna. Many telecommunication firms are looking into possible ways to lower the SAR value that mobile phone customers are exposed to by investigating the SAR's lowering in the mentioned frequency range. For immunology-telemetry applications, SAR has drawn increasing attention as more people become aware of the harmful effects of exposure to high-volume microwave waves. This could lead to hotspots in the body, which might result in tissue deterioration. In situations where antennas need to be placed close to the human body, such as in pagers, body-worn computers, body area networks [2, 3], or portable computers, a low SAR system would be perfect. Different kinds of RF-absorbing materials are deployed to fabricate RF shields. In this paper, foam and ferrite shields are considered due to their light weight and the fact that they do not cause signal degradation. The reduction of SAR utilizing RF shields is specified in terms of the SAR Reduction Factor (SRF).

$$SRF = \frac{SAR \text{ Without shield} - SAR \text{ With shield}}{SAR \text{ Without shield}} * 100 \quad (1)$$

II. HARMFUL EFFECTS OF THE 5G TECHNOLOGY ON HUMAN HEALTH

Worldwide, governments helped telecommunication businesses deploy 5G technology. It was first applied in China before spreading to the USA, Europe, and other industrialized nations. In 5G, every person on earth has access to a constant, low-latency, high-speed wireless connection that is connected to the public internet. The primary issue that entire nations overlook is the former's detrimental impact on the environment [4]. Sub-mmW and mmW, which operate in the 6GHz to 100GHz frequency range (used by 5G infrastructure), are unable to travel over longer distances and have limited solid-state penetration capabilities. Strong electromagnetic fields (EMFs) created by 5G mobile devices induce skin rashes, tissue heating, and burning [5]. Despite the fact that no study has established that exposure to 5G radiation causes skin rashes, numerous studies have demonstrated that the particular technology has negative impact on human body heat and skin tissue. Millimeter waves can penetrate the skin up to 1.0 mm, according to tight guidelines given to all service providers by the International Telecom Union. 3G technology ushered in a new era in wireless networking development. Various technologies were implemented throughout this age, ranging from multimedia technology to high-speed data transfer. During this time, a considerable number of base stations were employed to improve end-user connectivity and multimedia services. Depending on the population density in the location, there are strict ICNIRP guidelines for service providers. EMF-RF exposure has both immediate and long term consequences. According to studies, the impact of radiation causes behavioral abnormalities and slows brain growth in children [6, 7]. Also, 5G radiation has lower penetrating power on the human body. 5G networks use mmW for communication, which have a limited range and penetration power. That is, the latter can penetrate up to 0.41 mm deep into skin at a 42 GHz band frequency. However, 4G radiation is able to penetrate human skin to a depth of 1 mm [8, 9]. The energy absorbed by 5G radiation is exceptionally high, because the 5G network employs mmW, which exhibit reduced thermal penetration capabilities, yet readily permeate the human skin when combined with perspiration [10].

III. PROPOSED PIF ANTENNA IMPLEMENTATION WITH RF SHIELDS

Figure 1 depicts the building of the suggested PIF antenna. The thin dielectric substrate Rogers RT duroid -5880, with a permittivity of 2.2 and a loss tangent of 0.0009, is placed above the radiating patch. The suggested antenna has overall dimensions of 12 mm × 18 mm, with λ_0 being the free-space wavelength at the resonant frequency of 26 GHz. A coaxial feed inner conductor is connected to the antenna's top radiating element, PEC. Conventional PIF antenna structures are designed on partial ground surfaces to increase bandwidth but the proposed PIFA structure is designed on a Full GND structure to improve gain values. In the proposed design, the PIFA geometry is kept undisturbed, i.e. it has a proper F structure. The two 'F' structures become part of the antenna and are combined by a semi-circular transmission line with a radius of 5 mm that feeds the PIF antenna structure.

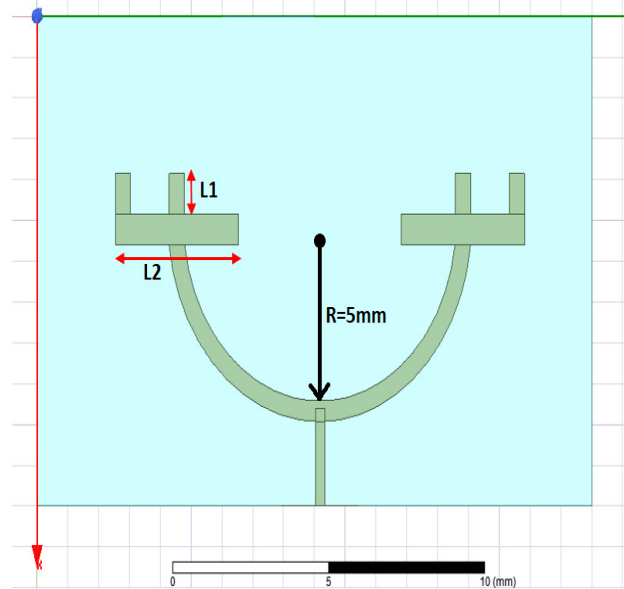


Fig. 1. The proposed PIF antenna.

$$f = \frac{c}{4(L1+L2)} \quad (2)$$

$$L1 \approx \frac{\gamma d}{4} = \frac{1}{4} \frac{c}{f \sqrt{\epsilon_r}} \quad (3)$$

$$L2 = \frac{c}{4f} \sqrt{\frac{2}{\epsilon_r + 1}} \quad (4)$$

According to (2), the PIFA length has an inverse relationship with the resonant frequency. Equations (3) and (4) can be used to determine the length of the PIFA section. In order to develop the proposed antenna, the following formulae were utilized. The computed value served as an initial PIFA dimension. In this computation, the operational frequency, f , is 26 GHz. To get the overall length, the formula in (5), is substituted. It is possible to determine the PIFA's length and breadth, $L1$ and $L2$, by:

$$f = \frac{c}{4(L1+L2)} \quad (5)$$

Referring to the distance between the two elements, the semi-circular disk is calculated as follows:

$$R = (\lambda/2) = 0.011/2 = R = 5 \text{ mm} \quad (6)$$

The dimensions of the proposed antenna are summarized in Table I.

IV. IMPACT OF RF SHIELDS ON REDUCING SPECIFIC ABSORPTION RATE IN 5G NETWORKS

The utilization of mmW at higher frequencies is a major innovation that will distinguish 5G networks from other cellular networks. Problematically, these waves cannot cover the same ground as their low-frequency counterparts. Telecommunication providers are responding by developing a denser network of tiny cells.

TABLE I. DIMENSIONS OF THE PROPOSED PIFA ANTENNA WITH RF SHIELDS

Parameter	Dimensions
Length	12 mm
Width	18 mm
Height of the substrate	0.8 mm
Substrate	Rogers RT duroid 5880
Substrate dielectric constant	2.2
Loss tangent	0.0009
Ground plane length	12 mm
Ground plane length	18 mm
Short pin width	0.5 mm
Number of locations in ferrite sheet attached in design	2
Ferrite sheet Dimensions (length×width)	3 mm × 8 mm, 3 mm × 1 mm
Thickness of ferrite sheet	0.8 mm
Number of locations in foam absorber attached in design	2
Foam absorber dimensions(length×width)	3 mm × 8 mm, 3 mm × 1 mm
Thickness of foam absorber	0.8 mm

A local antenna inside a cell connects all 5G network devices to the internet and telephone network via radio waves, increasing the radiation levels as cell number increases. Effective reduction in radiation can be achieved with the use of suitable RF shielding materials. Developing shielding materials [11, 12] with unique electromagnetic characteristics can address the issue of high frequency electromagnetic fields in the microwave region and their potentially detrimental effects on humans because these materials absorb and block electromagnetic radiation from microwaves. MI/RF shielding is a method of reducing electromagnetic fields by erecting barriers of conductive or magnetic materials to stop them. Applying shielding to mobile phones [13] allows them to absorb the radiation being delivered through the air. To ensure that mobile phones remain unaffected by outside electromagnetic radiation, certain RF shields must be adhered. As with previous generations, 5G uses RF shielding to achieve this. Metal shielding devices and conductive silicon and plastic devices are some of the shielding devices utilized in the electronic information system and mobile phone industries. Ferrite and foam absorber materials are employed as shield materials to reduce SAR. RF shields are attached to the front side of the mobile phones, suppressing the surface currents on the front side of the phone. RF shields absorb the EMW energy in the form of magnetic loss. Ferrite is the most commonly used material for reducing SAR. RF carbon foam is another form of EMI protection that is becoming increasingly popular, even though it does not contain metals. The EMI-protecting foam is effective from 100 MHz to 30 GHz. Because of its adaptability, foam excels as an EMI shield medium. Both materials have dimensions of 3 mm×8 mm (length and width) and 0.8 mm thickness and are attached in two locations on the proposed antenna. The impact of RF shields at higher frequencies (26 GHz) is not more than 4G LTE (2.4 GHz) because of the increased number of cells of the 5G Network.

A. Flexible Ferrite Sheet

In the high frequency band, energy absorption in ferrite sheets occurs due to dielectric loss. Charges are unable to pass

through dielectrics in an electric field. However, under the influence of an electric field, charge particles will displace from each other, leading to the separation of positive and negative charge centers and the formation of numerous electric dipoles. Shielding materials are typically defined by their electrical permittivity and magnetic permeability. These flexible ferrite sheets are composed of NiZn, which is ideal for high frequencies (mmW) because of its high resistance and excellent permeability. Extensive exposed areas of the extremely porous NiZn ceramics may have different spin orientations from the inner layers, which results in an adverse exchange effect in the NiZn body. The sheets are made with a 0.01 mm thick PET film on one side of the ferrite material and a 0.02 mm thick adhesive tape on the other side. The properties of the flexible ferrite sheet are incorporated in Table II.

TABLE II. PROPERTIES OF THE FLEXIBLE FERRITE SHEET

Properties	Value
Operating Temperature (°C)	-60 to +85
Permeability (μ')	20
Surface resistance	10^6
Dielectric constant	2.6
Feature	Silicon based
Operating frequency	30 MHz-40 GHz
Thickness	0.2 mm (total thickness-0.13mm)

B. Foam Absorber

Apart from reflection, electromagnetic wave absorption is an effective type of shielding, as the waves are absorbed into heat by the shielding material. The foam absorber is a high-performance absorber that operates in an ultra-wide frequency range, ranging from 30 MHz to 40 GHz. Tiny and lightweight, yet possessing excellent mechanical strength, this absorber is ideal for applications requiring monitoring of higher frequencies. Polyurethane (PU) is a prevalent environmentally friendly polymer known for its excellent tensile strength, flexibility, and mechanical characteristics. Fe_3O_4 @Polyvinyl alcohol (Fe_3O_4 @PVA) and GO@Ag were incorporated into the basic materials for preparing PU foam.

TABLE III. PROPERTIES OF FOAM ABSORBER

Properties	Value
Material	Fe_3O_4 @Polyvinyl alcohol
Absorption	60 dB at 18 GHz, 82 dB at 32 GHz, and 97 dB at 40 GHz
Operating frequency	18 GHz to 40 GHz
Thickness	0.8 mm
Dimensions	3 mm × 8 mm, 3 mm × 1 mm
Operating temperature	-50 to 90 °C

V. RESULTS AND DISCUSSION

To validate the design of the proposed antenna, a prototype was constructed. The antenna was simulated using ANSYS HFSS Software, Figures 2 and 3 show the fabricated prototype and the radiation pattern measurements in an anechoic chamber. The simulated and measured results for different parameters are presented in this section.

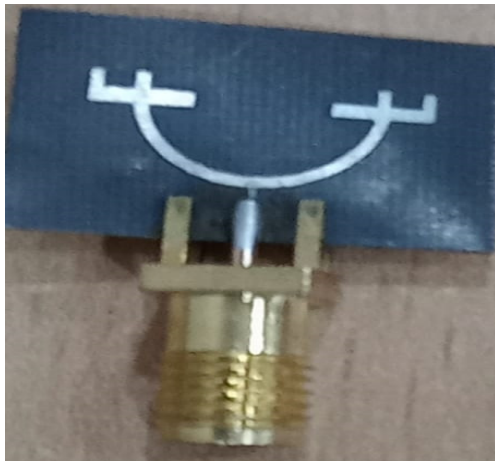


Fig. 2. Top view of the fabricated prototype.

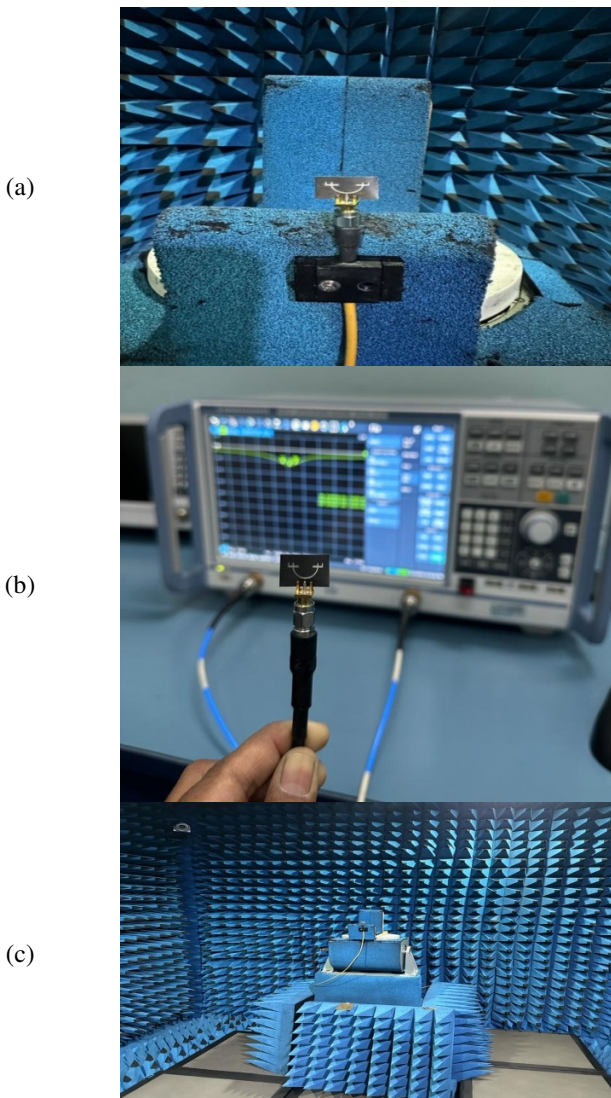


Fig. 3. (a) Testing of the proposed antenna in the anechoic chamber, (b) measurement setup of the proposed prototype in VNA, (c) front view of testing in the anechoic chamber.

A. Return Loss

Figure 4 exhibits the return loss of the proposed PIF antenna with no shielding material attached. The simulated S11 of the proposed antenna at 26 GHz is -16.26 dB. Figure 5 portrays the return loss of the antenna with ferrite sheet attachment for reducing SAR. The simulated value at 26 GHz is -13.10 dB. Figure 6 illustrates the simulation results of the return loss of the proposed antenna with a foam absorber shield. The acquired value at 26 GHz is -23.41 dB.

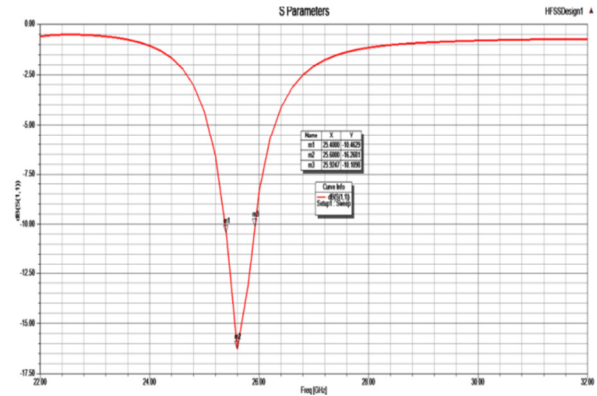


Fig. 4. S11 plot (without shield) @ 26GHz. Value: -16.26 dB.

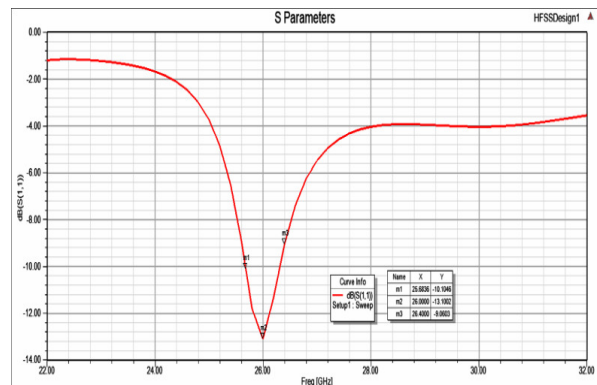


Fig. 5. S11 plot (with ferrite shield) @ 26GHz. Value: -13.16 dB.

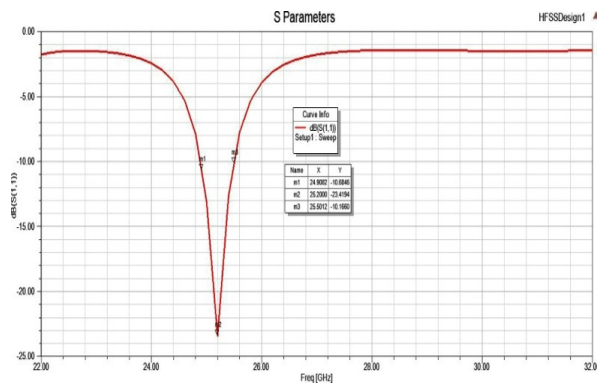


Fig. 6. S11 plot (with foam absorber shield) @ 26GHz. Value: -23.41 dB.

B. Gain

Figure 7 displays the gain of the proposed PIF antenna without any shielding material. The gain value measured is 5.60. A radiation pattern of a PIF antenna's signal as a function of the direction is facing away from the antenna. Figures 8 and 9 reveal the gain of the PIF antenna with ferrite sheet and foam absorber, respectively. The obtained gain at 26 GHz is 5.98 and 6.81, respectively.

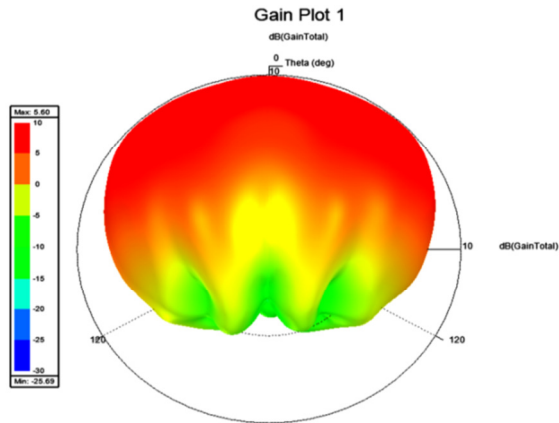


Fig. 7. 3D polar plot @ 25.6GHz. Gain: 5.6 dBi (no shield).

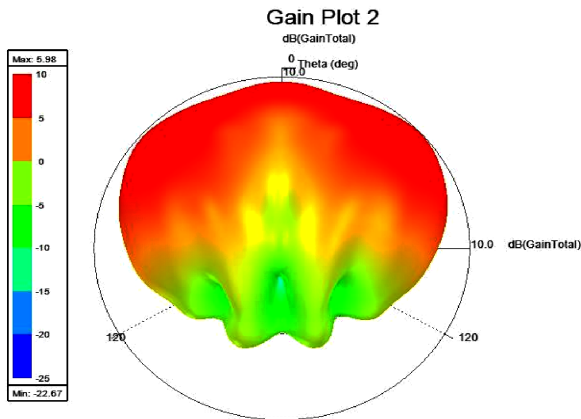


Fig. 8. 3D polar plot @ 25.6GHz. Gain: 5.9 dBi (ferrite shield).

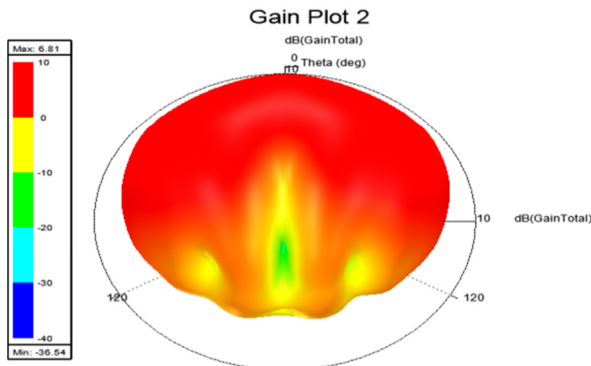


Fig. 9. 3D polar plot @ 25.6GHz. Gain: 6.81 dBi (foam absorber).

C. E & H Fields

Figures 10 and 11 disclose the E&H field distribution of the PIF antenna without any shielding material and Figures 12 and 13 depict the E&H fields with foam absorber and ferrite sheet, utilized as shields.

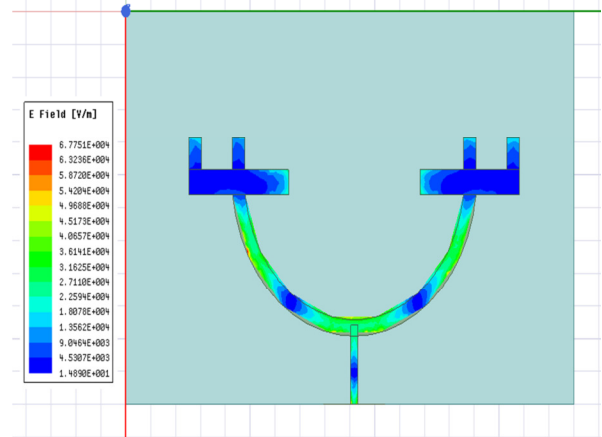


Fig. 10. Magnitude of E surface current distribution.

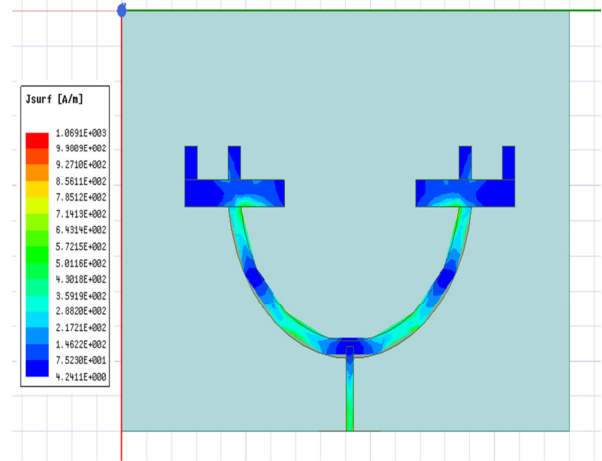


Fig. 11. Magnitude of J surface current distribution.

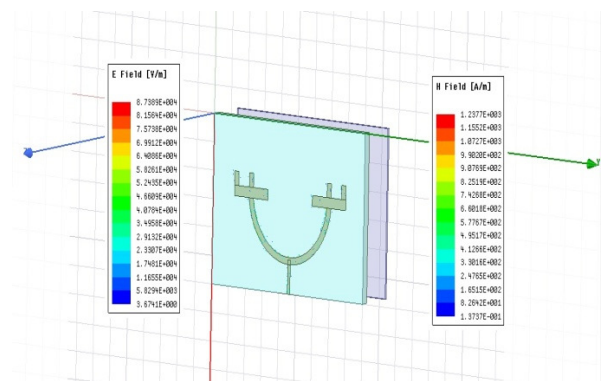


Fig. 12. E&H fields of the foam absorber.

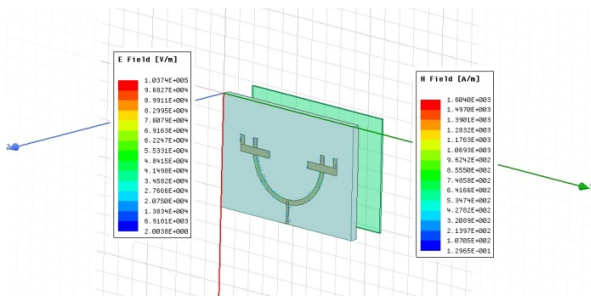


Fig. 13. E&H fields of the ferrite sheet.

D. SAR

Figures 14-16 demonstrate the measured values of the SAR of the proposed PIF antenna on a human head model (see also [18, 19]) without and with RF shields.

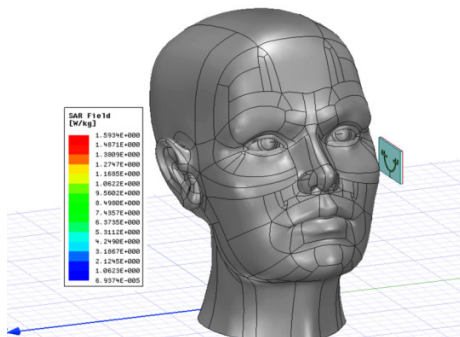


Fig. 14. SAR @26GHz is 1.59W/kg (without shield).

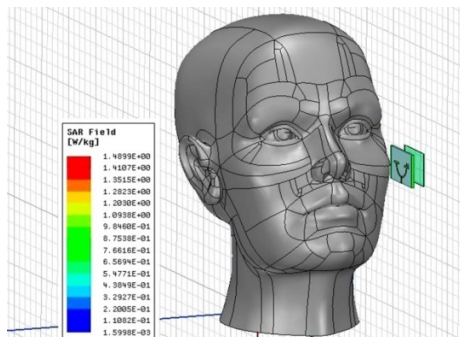


Fig. 15. SAR @26GHz is 1.48W/kg (with foam absorber shield).

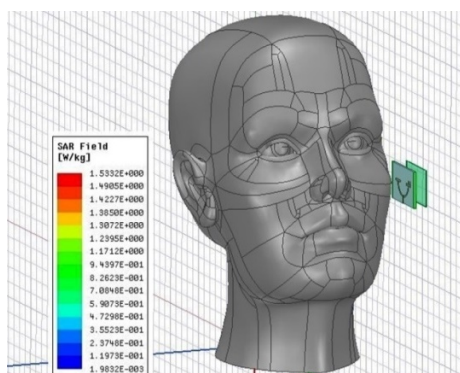


Fig. 16. SAR @26GHz is 1.53 W/kg (with ferrite shield).

TABLE IV. PROPOSED PIF ANTENNA PERFORMANCE COMPARISON WITHOUT AND WITH SHIELDS (26GHZ)

Parameter	Without shield	With ferrite sheet	With foam absorber
Return Loss	-16.26	-13.10	-23.41
Gain (dB)	5.60	5.98	6.81
Bandwidth (GHz)	0.52	0.8	0.7
SAR (W/Kg)	1.59	1.53	1.48
SRF (%)		3.7%	7%

TABLE V. COMPARISON OF THE PROPOSED ANTENNA WITH EXISTING WORKS

Ref	Antenna dimensions (mm)	Operating frequency (GHz)	SAR (W/kg)
[14]	14.76 × 8.33 (planar dipole)	28	0.963
[15]	29 × 52	27-29.5	1.81
[7]	147 × 70	28	1.59
[16]	14 × 28	4.858	1.26
[17]	9.3 × 9.3 × 0.254	28	1.34
Proposed	12 × 18	26	1.48

VI. CONCLUSION AND FUTURE WORK

A novel Planar Inverted F-Antenna (PIFA) structure designed to operate at 26 GHz, incorporating RF shields in the form of ferrite and foam absorber, is introduced in this study. The simulation results for the proposed design (return loss, gain, and bandwidth) at the specified frequency were presented and analyzed. The antenna size is smaller than that of previous works and the distance between the human head model and the proposed antenna is 5 mm. The inclusion of RF shields is observed to lead to a substantial reduction in Specific Absorption Rate (SAR) values. The comparative analysis of the results indicates that at 5G frequencies, foam absorbers outperform ferrite as effective RF shields. This is evident in achieving better SAR values and other pertinent parameters. The findings affirm the efficacy of the proposed antenna structure in increasing gain and mitigating SAR, with the foam absorber emerging as a particularly promising RF shielding material. SRF values can be improved by increasing the distance between the human head and the mobile antenna.

In order to expand this work, thermal analysis can be conducted by measuring the temperature rise at each human head tissue at short term (seconds) and long term (minutes) at 5G networks (more than 26 GHz). For measurements of real SAR values, the human head was modeled with liquid, so the obtained results are not accurate.

REFERENCES

- [1] J. G. Melekoodappattu, P. Dhanesh, and A. Kadan, "A Review on SAR Reduction Methods Used For Mobile Application," vol. 10, pp. 25–27, Sep. 2015.
- [2] W. Bouamra, I. Sfar, A. Mersani, L. Osman, and J. M. Ribero, "A Low-Profile Wearable Textile Antenna Using AMC for WBAN Applications at 5.8GHz," *Engineering, Technology & Applied Science Research*, vol. 12, no. 4, pp. 9048–9055, Aug. 2022, <https://doi.org/10.48084/etasr.5011>.
- [3] H. Yalduz, T. E. Tabaru, V. T. Kilic, and M. Turkmen, "Design and analysis of low profile and low SAR full-textile UWB wearable antenna with metamaterial for WBAN applications," *AEU - International Journal of Electronics and Communications*, vol. 126, Nov. 2020, Art. no. 153465, <https://doi.org/10.1016/j.aeue.2020.153465>.

- [4] C. Y. Chiu, K. M. Shum, C. H. Chan, and K. M. Luk, "Bandwidth enhancement technique for quarter-wave patch antennas," *IEEE Antennas and Wireless Propagation Letters*, vol. 2, pp. 130–132, 2003, <https://doi.org/10.1109/LAWP.2003.816636>.
- [5] S. S. Pudipeddi and P. V. Y. Jayasree, "Investigation of the Effect of Normal Incidence of RF Wave on Human Head Tissues Employing Cu and Ni Grid PET Films," *Engineering, Technology & Applied Science Research*, vol. 12, no. 6, pp. 9445–9449, Dec. 2022, <https://doi.org/10.48084/etasr.5252>.
- [6] S. S. Pudipeddi, P. V. Y. Jayasree, and S. G. Chintala, "Polarization Effect Assessment of Sub-6 GHz Frequencies on Adult and Child Four-Layered Head Models," *Engineering, Technology & Applied Science Research*, vol. 12, no. 4, pp. 8954–8959, Aug. 2022, <https://doi.org/10.48084/etasr.5096>.
- [7] M. S. Morelli, S. Gallucci, B. Siervo, and V. Hartwig, "Numerical Analysis of Electromagnetic Field Exposure from 5G Mobile Communications at 28 GHz in Adults and Children Users for Real-World Exposure Scenarios," *International Journal of Environmental Research and Public Health*, vol. 18, no. 3, Jan. 2021, Art. no. 1073, <https://doi.org/10.3390/ijerph18031073>.
- [8] R. Kumar, R. Geleta, A. Pandey, and D. Sinwar, "Adverse Effects of 5th Generation Mobile Technology on Flora and Fauna: Review Study," *IOP Conference Series: Materials Science and Engineering*, vol. 1099, no. 1, Mar. 2021, Art. no. 012031, <https://doi.org/10.1088/1757-899X/1099/1/012031>.
- [9] T. Hamed and M. Maqsood, "SAR Calculation & Temperature Response of Human Body Exposure to Electromagnetic Radiations at 28, 40 and 60 GHz mmWave Frequencies," *Progress In Electromagnetics Research M*, vol. 73, pp. 47–59, 2018, <https://doi.org/10.2528/PIERM18061102>.
- [10] M. Tamim, M. R. I. Faruque, M. U. Khandaker, M. T. Islam, and D. A. Bradley, "Electromagnetic radiation reduction using novel metamaterial for cellular applications," *Radiation Physics and Chemistry*, vol. 178, Jan. 2021, Art. no. 108976, <https://doi.org/10.1016/j.radphyschem.2020.108976>.
- [11] P. Chaudhary and R. Vijay, "Calculation of SAR on Human Brain Model and Analysis of the Effect of Various Dielectric Shielding Materials to Reduce SAR," in *International Conference on Intelligent Computing and Smart Communication 2019*, Singapore, 2020, pp. 545–550, https://doi.org/10.1007/978-981-15-0633-8_53.
- [12] L. H. Hemming, *Architectural Electromagnetic Shielding Handbook: A Design and Specification Guide*, 1st edition. Wiley-IEEE Press, 2000.
- [13] P. K. Dutta, P. V. Y. Jayasree, and V. S. N. S. Baba, "SAR reduction in the modelled human head for the mobile phone using different material shields," *Human-centric Computing and Information Sciences*, vol. 6, no. 1, Apr. 2016, Art. no. 3, <https://doi.org/10.1186/s13673-016-0059-0>.
- [14] R. H. Elabd and A. J. A. Al-Gburi, "SAR assessment of miniaturized wideband MIMO antenna structure for millimeter wave 5G smartphones," *Microelectronic Engineering*, vol. 282, no. C, Oct. 2023, Art. no. 112098, <https://doi.org/10.1016/j.mee.2023.112098>.
- [15] A. Lak, Z. Adelpour, H. Oraizi, and N. Parhizgar, "Design and SAR assessment of three compact 5G antenna arrays," *Scientific Reports*, vol. 11, no. 1, Oct. 2021, Art. no. 21265, <https://doi.org/10.1038/s41598-021-00679-8>.
- [16] T. Ramachandran, M. R. I. Faruque, A. M. Siddiky, and M. T. Islam, "Reduction of 5G cellular network radiation in wireless mobile phone using an asymmetric square shaped passive metamaterial design," *Scientific Reports*, vol. 11, no. 1, Jan. 2021, Art. no. 2619, <https://doi.org/10.1038/s41598-021-82105-7>.
- [17] J. Khan, D. A. Sehrai, and U. Ali, "Design of Dual Band 5G Antenna Array with SAR Analysis for Future Mobile Handsets," *Journal of Electrical Engineering & Technology*, vol. 14, no. 2, pp. 809–816, Mar. 2019, <https://doi.org/10.1007/s42835-018-00059-9>.
- [18] S. S. Pudipeddi, P. V. Y. Jayasree, and S. G. Chintala, "Polarization Effect Assessment of Sub-6 GHz Frequencies on Adult and Child Four-Layered Head Models," *Engineering, Technology & Applied Science Research*, vol. 12, no. 4, pp. 8954–8959, Aug. 2022, <https://doi.org/10.48084/etasr.5096>.
- [19] I. Androulidakis and G. Kandus, "Mobile Phone Brand Categorization vs. Users' Security Practices," *Engineering, Technology & Applied Science Research*, vol. 1, no. 2, pp. 30–35, Apr. 2011, <https://doi.org/10.48084/etasr.19>.